

Liver Tumor Gross Margin Identification and Ablation Monitoring during Liver Radiofrequency Treatment

Christopher P. Hsu, MD, Mahmood K. Razavi, MD, Samuel K. So, MD, Ilian H. Parachikov, and David A. Benaron, MD

PURPOSE: To determine whether tissue visible light spectroscopy (VLS) used during radiofrequency (RF) ablation of liver tumors could aid in detecting when tissue becomes adequately ablated, locate grossly ablated regions long after temperature and hydration measures would no longer be reliable, and differentiate tumor from normal hepatic tissue based on VLS spectral characteristics.

MATERIALS AND METHODS: Studies were performed on human liver *in vivo* and animal liver *ex vivo*. In three *ex vivo* cow livers, RF-induced lesions were created at 80°C. A 28-gauge needle embedded with VLS optical fibers was inserted alongside an RF ablation array, and tissue spectral characteristics were recorded throughout ablation. In one anesthetized sheep *in vivo*, a VLS needle probe was passed through freshly ablated liver lesions, and ablated region spectral characteristics were recorded during probe transit. In two human subjects, a VLS needle probe was passed through liver tumors in patients undergoing hepatic tumor resection without ablation, and tumor spectral characteristics were recorded during probe transit.

RESULTS: In bovine studies, there was significant change in baseline absorbance ($P < .0001$) as a result of increased light scattering as liver was ablated. Liver exhibited native differential absorbance peaks at 550 nm that disappeared during ablation, suggesting that optical spectroscopy detects markers of tissue altered during ablation. In sheep, liver gross ablation margins were clearly defined with millimeter resolution during needle transit through the region, suggesting that VLS is sensitive to gross margins of ablation, even after the temperature has normalized. In humans, absorbance decreased as the needle passed from normal tissue into tumor and normalized after emerging from the tumor, suggesting that absence of native liver pigment may serve as a marker for the gross margins and presence of tumors of extrahepatic origin.

CONCLUSIONS: In human subjects, VLS during RF liver tumor ablation depicted gross hepatic tumor margins in real time; in animal subjects, VLS achieved monitoring of when and where RF ablation endpoints were achieved, even long after the tissue cooled. Real-time *in vivo* monitoring and treatment feedback may be possible with the use of real-time VLS sensors placed along side of, or embedded into, the RF probe, which can then be used as an adjunct to standard imaging during tumor localization and RF ablation treatment.

J Vasc Interv Radiol 2005; 16:1473-1478

Abbreviations: RF = radiofrequency, MR = magnetic resonance, US = ultrasound, VLS = visible light spectroscopy

PERCUTANEOUS radiofrequency (RF) ablation is an emerging palliative treat-

ment for advanced hepatic carcinoma, most commonly arising from metastatic

adenocarcinoma (1). The primary mode of tumor destruction is a thermal coagulation necrosis (2). Unfortunately, even with intraprocedural monitoring, coagulation necrosis does not lend itself to quantitative, real-time feedback. First, it is difficult to assess when the RF electrode properly encompasses the tumor. Second, when multiple and overlapping ablation treatments are planned to treat a large or irregularly shaped tumor, the gross margin of destruction is poorly visualized by current intraoperative imaging methods.

From Santa Clara Valley Medical Center (C.P.H.), San Jose; Department of Interventional Radiology (M.K.R.), Department of General Surgery (S.K.S.), and Department of Pediatrics (D.A.B.), Stanford University Medical Center, Palo Alto; and Spectros Corporation, Portola Valley, California. Received November 1, 2004; revision requested December 22; revision received and accepted July 8, 2005. **Address correspondence** to D.A.B., 4370 Alpine Rd., Suite 108, Portola Valley, CA 94028; E-mail: dbenaron@spectros.com.

M.K.R. is a member of the Spectros Corporation Advisory Board and receives equity compensation. I.P. and D.A.B. are Employees of Spectros Corporation and receive financial and equity compensation. None of the other authors have identified a conflict of interest.

© SIR, 2005

DOI: 10.1097/01.RVI.000017833.30967.39

To monitor the adequacy of ablation, two endpoints have been commonly used: (i) documentation of tissue temperature or impedance-determined hydration status during and immediately after ablation and/or (ii) definition of the extent of coagulation tissue with imaging (3). With regard to temperature, sensors can be inserted into the ablation site to measure focal point temperatures and magnetic resonance (MR) thermometry have been shown to correlate with temperature in rabbits. Similarly, impedance is a reflection of tissue hydration status during and after ablation. However, temperature and water content change with time after ablation, limiting the utility of these values in clinical practice (4,5). With regard to imaging, many imaging strategies have been evaluated with limited success, including MR or computed tomography with or without contrast agent enhancement (3), hyperechogenicity with ultrasonography (US), optical coherence tomography (6,7), and electrical impedance tomography (8).

The inability to perform accurate, predictive, real-time intraoperative ablation monitoring reduces the efficacy of the procedure, lengthens treatment times, and forces extensive postprocedural imaging and follow-up to evaluate tumor destruction. In addition, follow-up imaging to determine the extent of residual or recurrent tumor is less than ideal.

Light-based tissue spectroscopy has been proposed for use as an ablation endpoint (9,10). It is known that in vivo optical properties reflect tissue structure (cell shape and number), tissue composition (concentration-dependent chemical absorbance), and tissue function (hemoglobin, myoglobin, and cytochrome oxygenation states).

The purpose of the present study was to determine if visible light tissue spectroscopy could be used during ablation of liver tumors to (i) aid in determining when tumors were adequately ablated, (ii) differentiate between tumor and normal tissue based on spectral signatures, and (iii) locate ablated regions long after temperature and hydration measures would have become unreliable. Our hypothesis was that the chemical and structural changes undergone by tissue during thermal ablation, which are

sufficient to be seen clearly by the naked eye after the liver is resected and sectioned, can provide a reliable signal for quantitative, real-time feedback during the ablation process.

MATERIALS AND METHODS

Visible Light Spectroscopy Monitor

The visible light spectroscopy (VLS) monitor consisted of a 28-gauge fiber-embedded needle (FireFly; Spectros, Portola Valley, CA), which has been described previously (11), connected to a Food and Drug Administration-approved VLS monitor (TStat; Spectros) in which white light from a probe placed on, in, or near tissue is used to illuminate the tissue under study. A fiberoptic strand in the needle collects light returning to the probe. The volume of sample of the needle is approximately 125 μL located forward of the tip of the needle. Tissue contact is not required for the VLS measurement. The VLS monitor separates collected light by wavelength into 2,048 bins, measured simultaneously (12). The TStat monitor was used in research mode to collect all spectral data recorded from the tissue during the ablation procedure.

Ablation Monitoring Ex Vivo

Fourteen ex vivo bovine livers weighing an average of 2 kg were studied. A multiple-tip RF ablation device (Starburst; Rita, Fremont, CA) was used for the ablation procedure. This probe was inserted into ex vivo liver and deployed alongside a 28-gauge fiber-embedded needle (Fig 1) parallel to but without contact with the Rita probe and fiber-embedded needle. The fiber-based needle was connected to the VLS monitor as described earlier. The Rita probe has multiple temperature-monitoring thermistors, including a thermistor located on the end of the central tine nearest the fiber probe. Ablation was performed according to standard treatment protocols beginning at 24°C to a maximum temperature of 80°C, as measured by temperature sensors embedded on the Starburst probe (Fig 2). The temperature at the central tine closest to the fiber probe was used for temperature correlation. All ablation performed reached target ablation temperatures,

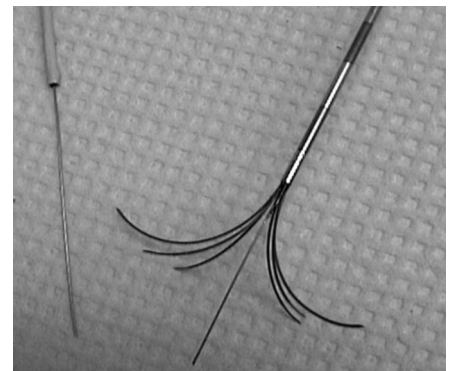


Figure 1. Left: Prototype 10-cm, 28-gauge solid needle embedded with optical fibers for real-time spectroscopy. Right: Multiple-tip RF ablation device.

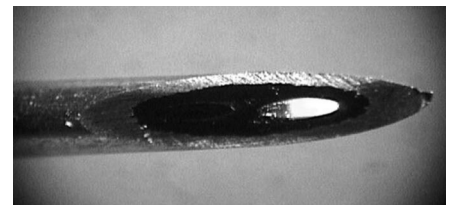


Figure 2. Close-up of needle tip with embedded emitter (bright) and detector (dark) fibers.

and the procedures were terminated 10 minutes after the target temperatures were reached. Real-time ablation spectra were recorded from 375 nm (ultraviolet) to 900 nm (infrared) at a rate of one full spectrum per second, which resulted in approximately 8,000 data points per sample. All data points for a given temperature were averaged to provide the result graphs. The absorbance spectra were calibrated and referenced to a lipid suspension (2% Intralipid solids [Pharmacia, Clayton, NC] in saline solution by weight). Calibration against the lipid suspension was performed before VLS use and provided a constant extinction coefficient throughout the entire experiment. Spectral raw data were saved to disk under personal computer control. Temperature readings from the thermistor within the RF device were also recorded, and time was correlated with the saved spectra (Figs 3,4).

Ablation Localization In Vivo

One sheep weighing approximately 50 kg was used and the procedure was

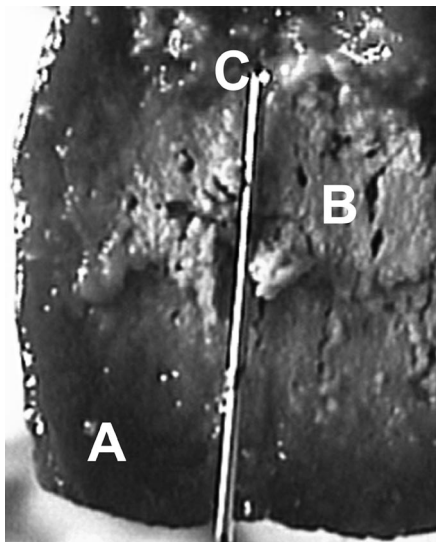


Figure 3. Bovine liver cross-section obtained after optically monitored ablation showing (A) a deep brown unablated area, (B) a pale central ablated area, and (C) the VLS probe in situ.

performed under general anesthesia. Induction of anesthesia was achieved with an intramuscular injection of 100 mg of ketamine hydrochloride. The animal was intubated and 1.0%–2.0% halothane was administered via endotracheal tube at a rate of 10 L/min. The animal was placed in the supine position after adequate anesthesia was achieved; the right upper quadrant and epigastrium were shaved, and the surface was sterilized. One thigh was shaved and the grounding pad was placed. A Starburst multiple-tip RF ablation device was used and ablation was performed according to standard treatment protocols to a maximum temperature of 80°C, as measured by temperature sensors embedded on the Starburst probe. After ablation, a 28-gauge fiber needle embedded with a VLS emitter and receiver was placed through the original ablation tract under US guidance. Real-time ablation spectra were recorded from 375 m to 900 m at a rate of one full spectrum per second as the probe was inserted in a continuous motion. Depth was estimated by correlating the time of the sample with the crossing of markings on the side of the VLS needle, with interpolation between distance marks. Similar to the aforementioned bovine liver ablation monitoring study, the probes were calibrated as before. Ap-

proval for this study was obtained from the animal institutional review board.

Tumor Localization In Vivo

Approval for this study was obtained from the institutional review board, with written informed patient consent obtained prior to each study. Two human subjects, 69 and 72 years old respectively, were studied. Both patients were undergoing scheduled liver resection for metastatic colorectal adenocarcinoma. Spectra were obtained as a fiber-enabled needle was inserted into the liver under US guidance. Later, pathology correlation was made to correlate probe depth with tumor location. Real time ablation spectra were recorded from 375 urn to 900 urn at a rate of one full spectrum per second. Again, needle depth was estimated by correlating the time of the sample with the crossing of markings on the side of the VLS needle, with interpolation between distance marks. Similar to the previous studies, the probes were calibrated against a lipid solution, and all spectral data were saved to disk.

Statistics

Mean and SD values were calculated from each data set. The normal distribution of optical values in tissue had been previously demonstrated. A small-sample two-tailed *t* test was applied to determine differences between mean values for baseline and peak absorbance values at different temperatures, with SD values based on intrasample variability with repeated measures.

RESULTS

Ablation Monitoring Results

Pooled spectra obtained from bovine liver during RF ablation are shown in **Figure 4**. There was a significant change in baseline absorbance during ablation. Absorbance at 700 nm decreased from -0.66 ± 0.03 at 27°C to -1.29 ± 0.01 at 79°C ($P < .0001$).

An absorbance peak at 555 nm was observed at all temperatures. At 27°C, the absorbance at this peak was -0.13 (relative to the lipid standard). This absorbance decreased as the tissue

temperature increased, from -0.25 at 45°C to -0.60 at 65°C and then to -0.87 at 73°C. Finally, at that temperature, the absorbance peak stabilized and remained at -0.87 as the tissue temperature increased from 73°C to 79°C. A decreased absorbance indicates that the tissue is becoming more optically reflective as it thermally denatures, whereas a stable absorbance at the highest temperature range suggests that the denaturation process has completed and the thermal endpoint has been reached.

Ablation Localization Results

A typical plot of absorbance at one wavelength, obtained as the needle passed into and through an ablated liver section, is shown in **Figure 5a**. There was a stable baseline absorbance in the infrared (870 nm, 0.39 ± 0.01) and visible (490 nm, 0.48 ± 0.01) wavelengths while traversing intact native liver; however, when the needle was advanced into region of ablated liver (at approximately 9.5 cm depth), the relative absorbance decreased to -0.30 ± 0.00 (870 nm; $P < .0001$) and -0.09 ± 0.00 (490 nm; $P < .0001$), each of which represents a fourfold increase in reflective intensity at the respective wavelengths (given the base-10 logarithmic scale of absorbance).

Both regions of increased reflectance corresponded with the gross location and size of the ablation area as measured photographically when the tissue was sectioned after completion of the study. This suggests that the gross margins of ablated regions, and the maximum temperature reached, can be mapped with use of VLS spectroscopy after the ablation has been completed.

Tumor Localization Results

A typical plot of first-derivative differential absorbance, obtained as the needle passed into and through a colorectal metastasis in human liver, is shown in **Figure 5b**. There was a stable maximum absorbance as the needle traversed intact, native liver, with a differential absorbance of 0.96 ± 0.00 at 650 nm; however, when the needle advanced into regions of metastatic cancer (at approximately 9 mm depth), the differential absorbance decreased

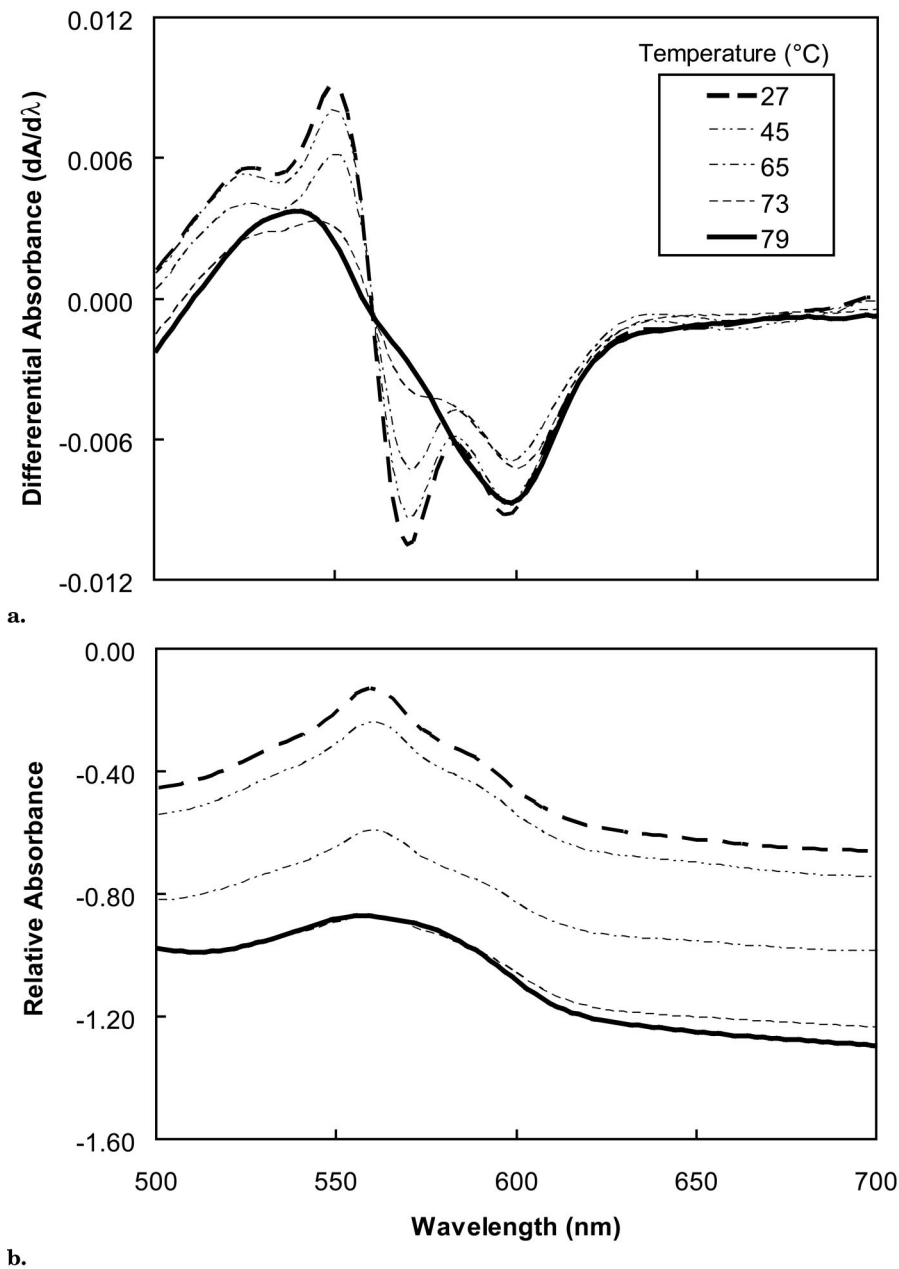


Figure 4. Changes in tissue absorbance over the visible wavelength range during RF ablation. **(a)** With absorbance plotted in first differential absorbance, which reduces the effect of tissue coupling and light scattering, some peaks appear to be destroyed during heating while others are thermostable. The stable peak does not correspond to known hemoglobin species. **(b)** Absorbance plotted as effective absorbance, in which changes in tissue scattering with temperature dominates the baseline, especially above 650 nm. Scattering increases with temperature, depressing the baseline effective absorbance, as the tissues are thermally ablated.

to -0.03 ± 0.00 ($P < .001$). The differential absorbance was stable throughout the tumor until the VLS needle passed through the posterior margin of the tumor, returning to a greater value after emerging from the distal

margin of the tumor at approximately 25 mm depth. With deeper insertion, differential absorbance returned to within 0.08 absorbance units of that of normal liver parenchyma. This suggests that the gross margins of meta-

static liver tumors (ie, of extrahepatic origin) can be mapped with use of VLS spectroscopy with millimeter precision.

DISCUSSION

This study demonstrates that tissue undergoes optical changes with ablation and that these changes may allow for measurements of the degree and extent of ablation that is detectable with VLS, even after the tissue has cooled. Persistence of the ablation measures is not a feature of previous measures such as electrical resistance or temperature. In addition, the optical differences between native liver and metastatic tumors may allow for the detection and localization of hepatic tumors with precise real-time localization of gross tumor margins. Together, this may allow for ablation to be better controlled and targeted with use of optical VLS feedback.

Previous work by Otten et al (9) looked at changes in light scattering by tissue ex vivo during cryoablation and showed that noninvasive optical imaging is possible, whereas Swartling et al (13) looked at changes in myocardial tissue light absorbance during ablation in pigs and found that metmyoglobin, formed in ablated tissue, could yield a spectral marker of ablation. Others have looked at changes well into the infrared spectrum, where protein chemistry and absorbance lines can be explored and exploited (14). Some groups are investigating the use of light to image ablation progress. For example, optical coherence tomography, an imaging technology, has been suggested in monitoring tissue ablation (6,7).

This study differs in several ways from previous studies. First, in the present study, visible light spectroscopy was employed to demonstrate that the absorbance spectra for each temperature allows for differentiation of maximum temperature reached, which may result in algorithms reflecting the tissue viability. Unlike temperature monitoring with use of thermistor probes or measurement of tissue hydration, which reflect temporary effects of ablation, the persistent measures used herein may allow the damage to be monitored well after the ablation has been completed. This would permit ablation probes to be

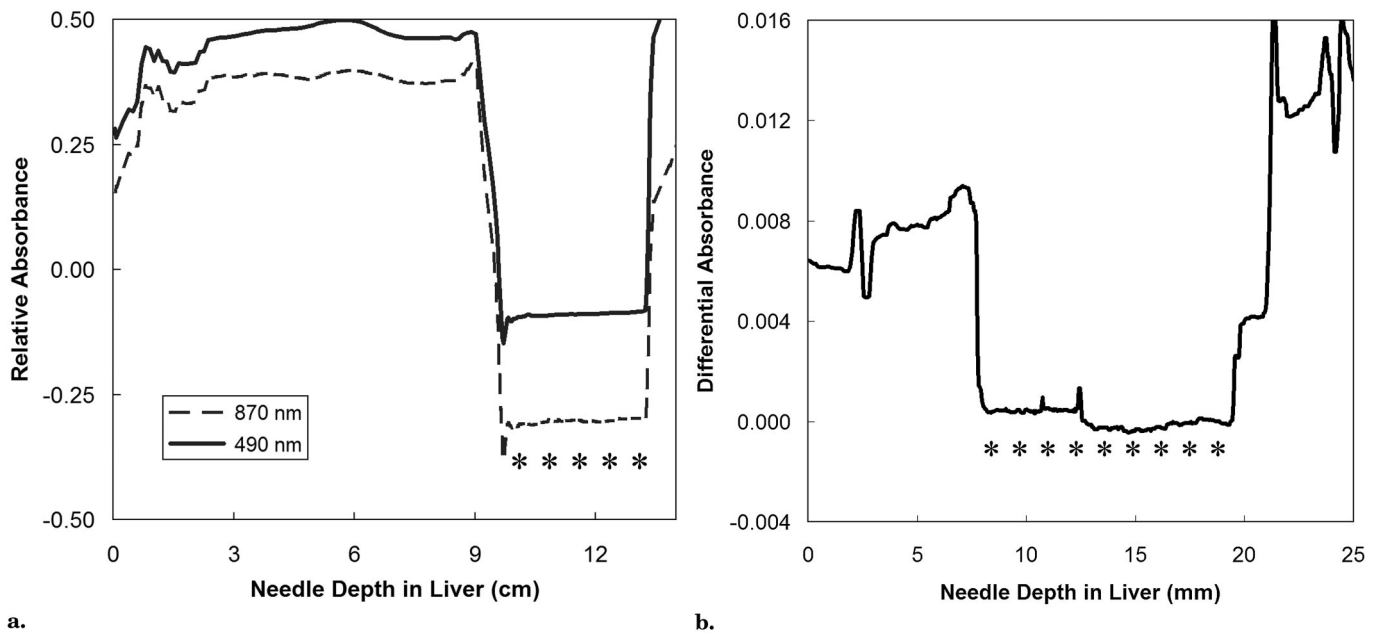


Figure 5. (a) Ablation Margin. Changes in absorbance at selected visible and infrared wavelengths as an optical needle approaches and passes through an ablated region in live ovine liver shortly after ablation. The gross margins of the ablated region are clear (asterisks). The local decreases in absorbance in ablated tissue are believed to arise from increases in tissue scattering during tissue destruction and may therefore serve as an indicator of tissue viability. **(b) Tumor Margin.** Changes in absorbance at one wavelength as an optical needle approaches and passes through hepatic tumors of extrahepatic origin in vivo in human subjects. The gross margins of the tumors are well delineated (asterisks). The local decreases in absorbance in this unablated tumor are believed to arise from the absence of primary liver pigments in these extrahepatic tumors.

repositioned minutes to hours after an ablation has been performed.

Second, during ablation, the liver spectra exhibited a well-defined first differential isosbestic point (the point at which the absorbance does not change with treatment) at 555 nm. Such an isosbestic point suggests an interconversion between two chemical species during ablation (15). Our analysis suggests that this is not a result of the generation of oxidized methemoglobin, as the 550 nm isosbestic point does not correlate with published isosbestic values for methemoglobin (16). This raises the possibility of a unique chemical marker for ablation progress and/or tissue viability.

Third, although decreased absorbance in the ablated regions was consistent with the findings of earlier studies that demonstrate a decrease in absorbance as tissue is ablated (17), the ability to localize this difference within millimeters suggests that an algorithm based on these values could result in stable, real-time tissue identification by distinguishing when the needle has passed through the ablated

tissue and entered back into normal tissue.

Last, the spectral characteristics of metastatic colorectal adenocarcinoma are markedly different than normal liver parenchyma and are within the sensitivity of the VLS probe, suggesting that an algorithm based on these values could result in possible tissue identification by distinguishing when the needle has passed through tumor and entered back into normal tissue.

The results agree with those of Swartling et al (13), who studied ablation in myocardial tissue and suggested that the optical properties described can be found in tissues other than liver. The results here are of interest in RF liver ablation, but from a broader perspective, they demonstrate the response of optical properties of tissue to heat-induced coagulation necrosis. The spectral composition of unablated tissue is measurably and significantly different than ablated tissue, suggesting the formation of new compounds that may serve as stable markers of ablation. As such, VLS may aid the interventionalist in determining when a particular level of ablation has

been reached. In addition, the results demonstrate that the spectral composition of colorectal adenocarcinoma is measurably different than liver tissue; specifically, colorectal adenocarcinoma demonstrates decreased relative absorbance (ie, increased reflectance) compared with liver tissue. This difference can be detected by the sensitivity of VLS probes embedded within the ablation instrumentation. The VLS technology, as deployed in a needle, can return data only along the needle tract. Three-dimensional data can be provided by incorporating the optical fibers into each RF ablation tine, as has been demonstrated in other multifiber optical imaging approaches (9,18), to allow mapping of the tumor (and ablation) during initial deployment, further trial extension of the tines, and retraction. Such a multifiber approach may further assist the interventionalist to immediately provide gross tissue characterizations in real time that augment the biopsy results that are usually available at a much later time.

We conclude that real-time VLS may aid the interventionalist in identifying gross tumor margins when a

percutaneous needle has entered tumor or liver tissue and for identifying when tissue at the site of the VLS probe has been ablated with RF, allowing for additional procedure feedback. Further study to evaluate the full clinical utility in image-guided tumor therapy is warranted. This may lead to a more reliable, reproducible, and safe procedure.

References

- Dodd GD III, Soulen MC, Kane RA, et al. Minimally invasive treatment of malignant hepatic tumors: at the threshold of a major breakthrough. *Radiographics* 2000; 20:9-27.
- Goldberg SN, Gazelle GS, Compton CC, et al. Treatment of intrahepatic malignancy with radio frequency ablation: radiologic pathologic correlation. *Cancer* 2000; 88:2452-2463.
- Goldberg SN, Dupuy DE. Image-guided radiofrequency tumor ablation: challenges and opportunities—part I. *J Vasc Interv Radiol* 2001; 12:1021-1032.
- Dickinson RJ, Hall AS, Hind AJ, et al. Measurement of changes in tissue temperature using MR imaging. *J Comput Assist Tomogr* 1986; 10:468-472.
- McDannold NJ, King RL, Jolesz FA, et al. Usefulness of MR imaging-derived thermometry and dosimetry in determining the threshold for tissue damage induced by thermal surgery in rabbits. *Radiology* 2000; 16:517-523.
- Boppart SA, Herrmann J, Pitris C, et al. High-resolution optical coherence tomography-guided laser ablation of surgical tissue. *J Surg Res* 1999; 82:275-284.
- Patel NA, Li X, Stamper DL, et al. Guidance of aortic ablation using optical coherence tomography. *Int J Cardiovasc Imaging* 2003; 19:171-178.
- Davalos R, Rubinsky B. Electrical impedance tomography of cell viability in tissue with application to cryosurgery. *J Biomech Eng* 2004; 126:305-309.
- Otten DM, Rubinsky B, Cheong WF, et al. Ice-front propagation monitoring in tissue by the use of visible-light spectroscopy. *Appl Optics* 1998; 37:6006-6010.
- Benaron DA, Goldberger DS, Goodman DE, et al. Device and method for analysis of surgical tissue interventions. United States Patent 5,762,609 (1998).
- Benaron DA, Parachikov IH, Cheong WF, et al. Quantitative, clinical, non-pulsatile, and localized visible light oximeter: design of the T-Stat tissue oximeter. *J Biomed Optics* 2005;10:1-9.
- Friedland S, Soetikno R, Benaron D. Reflectance spectrophotometry for the assessment of mucosal perfusion in the gastrointestinal tract. *Gastrointest Endosc Clin N Am* 2004; 14:539-553.
- Swartling J, Palsson S, Platonov P, et al. Changes in tissue optical properties due to radio-frequency ablation of myocardium. *Med Biol Eng Comput* 2003; 41:403-409.
- Spencer P, Payne JM, Cobb CM, et al. Effective laser ablation of bone based on the absorption characteristics of water and proteins. *J Periodontol* 1999; 70:68-74.
- Ahmed S, McPhie P, Miles E. A thermally induced reversible conformational transition of the tryptophan synthase $\alpha 2$ subunit probed by the spectroscopic properties of pyridoxal phosphate and by enzymatic activity. *J Biol Chem* 1996; 271:8612-8617.
- Zijlstra WG, Buursma A, van Assendelft OW. Visible and near infrared absorption spectra of human and animal haemoglobin. Utrecht, The Netherlands: VSP Publishing, 2000.
- Agah R, Gandjbakhche AH, Motamedi M, et al. Dynamics of temperature dependent optical properties of tissue: dependence on thermally induced alteration. *IEEE Trans Biomed Eng* 1996; 43:839-846.
- Benaron DA, Hintz SR, Villringer A, et al. Noninvasive functional imaging of the human brain using light. *J Cereb Blood Flow Metab* 2000; 20:469-477.